Backbone exponents of the two-dimensional q-state Potts model: A Monte Carlo investigation

Youjin Deng,[1] Henk W. J. Blöte,[1,2] and Bernard Nienhuis[3]
[1]*Faculty of Applied Sciences, Delft University of Technology, P.O. Box 5046, 2600 GA Delft, The Netherlands*
[2]*Lorentz Institute, Leiden University, P.O. Box 9506, 2300 RA Leiden, The Netherlands*
[3]*Institute of Theoretical Physics, University of Amsterdam, Valckenierstraat 65, 1018 XE Amsterdam, The Netherlands*
(Received 14 October 2003; published 26 February 2004)

We determine the backbone exponent X_b of several critical and tricritical q-state Potts models in two dimensions. The critical systems include the bond percolation, the Ising, the $q=2-\sqrt{3}$, 3, and 4 state Potts, and the Baxter-Wu model, and the tricritical ones include the $q=1$ Potts model and the Blume-Capel model. For this purpose, we formulate several efficient Monte Carlo methods and sample the probability P_2 of a pair of points connected via at least two independent paths. Finite-size-scaling analysis of P_2 yields X_b as 0.3566(2), 0.2696(3), 0.2105(3), and 0.127(4) for the critical $q=2-\sqrt{3}$, 1,2, 3, and 4 state Potts model, respectively. At tricriticality, we obtain $X_b=0.0520(3)$ and 0.0753(6) for the $q=1$ and 2 Potts model, respectively. For the critical $q\to 0$ Potts model it is derived that $X_b=3/4$. From a scaling argument, we find that, at tricriticality, X_b reduces to the magnetic exponent, as confirmed by the numerical results.

DOI: 10.1103/PhysRevE.69.026114 PACS number(s): 05.50.+q, 64.60.Cn, 64.60.Fr, 75.10.Hk

I. INTRODUCTION

The integer q-state Potts model [1] is an extension of the Ising model, and has been a subject of intense research interest for decades. It can be generalized to the random-cluster model of all $q\geqslant 0$ [2]. For a review see Ref. [3]. This model has been shown to be very rich in its behavior. In two dimensions, the nature of the critical singularities is now well established. In the study of critical phenomena, the Potts model has become an important testing ground for various methods and approaches.

However, there is still a number of critical exponents, of which the exact values have not been obtained. These exponents characterize geometric properties of the critical Potts models, and seem to have no analog in the thermodynamics. Among them there are fractal dimensions of ''backbones'' [4] and of ''chemical'' paths [5].

Here, we shall briefly review definitions of these quantities, in the language of the percolation model [6], a special case of the Potts model for $q\to 1$. Consider a bond percolation model on the square lattice; each edge of the lattice is occupied by a ''conducting'' bond with probability p, or is ''empty'' with probability $1-p$. At the critical point $p_c=1/2$ [6], a percolating cluster, which consists of sites connected via these conducting bonds, will grow arbitrarily large. Suppose one has a percolating cluster, which contains two sites S_1 and S_2 separated by a distance r. The backbone [4] is then defined as the set of sites from which conducting paths exist both to S_1 and S_2, such that both paths have no bonds in common, i.e., the paths are mutually independent. Thus, if a potential difference is applied to S_1 and S_2, the backbone consists exactly of those sites through which current would flow, apart from the so-called ''Wheatstone bridges.'' At criticality, the total number of sites or bonds in the backbone scales as $N_b\propto r^{d-X_b}$, where $d=2$ and X_b are the spatial and the backbone scaling dimension, respectively. The chemical path [5] is defined as the shortest path between S_1 and S_2. Its average length at criticality behaves as $l\propto r^{d-X_{\min}}$, with $X_{\min}$ the corresponding scaling dimension. Another exponent of interest is related to the so-called ''red'' bonds. Suppose a bond in the percolating cluster carries all the current and thus becomes ''hot'' after some time, then this bond is named a red bond [4,5]. A cluster with one or more red bonds will, if any red bond is cut off, split into disconnected subclusters. The total number of red bonds in the percolating cluster behaves as $N_r\propto r^{d-X_r}$, with X_r the red-bond scaling dimension.

As mentioned earlier, the ''geometric'' exponents, such as X_b, X_r, and $X_{\min}$, characterize geometric structures of critical systems, and are thus of some physical relevance. For instance, the backbone and red-bond scaling dimensions X_b and X_r are related to the electric conductivity of a random network [7]. The chemical-path dimension $X_{\min}$ is the analog in percolation of the dynamic scaling exponent of critical phenomena [8].

Among these exponents, the red-bond dimension X_r has been identified with another exponent X_p [9,10], which governs the renormalization flow of the bond probability p for critical systems. As a result, exact values of X_r can be calculated from the theory of the Coulomb gas [11]; these values are also included in the prediction of the conformal field theory [9,12,13]. However, except for the special case $q\to 0$, exact values have not been obtained for X_b and $X_{\min}$. Numerous theoretical attempts have been carried out. For the percolation model $q\to 1$, a relation was assumed by Herrmann and Stanley [14] as $X_b=X_r-X_{\min}$, which satisfies numerical tests quite well so far. However, this conjecture apparently cannot be generalized to the critical $q\to 0$ Potts model, where $X_b=X_r=X_{\min}$, as shown later. It was also assumed that $X_b(q\to 1)=7/16$ [15,16], which is, however, not consistent with current estimations. More recently, $X_b(q\to 1)$ has been related to a partial differential equation [17], which, unfortunately, appears to be intractable, even numerically.

In parallel with these theoretical attempts, several numerical determinations of X_b have been achieved. Significant progress is obtained by Monte Carlo simulations [8,14,18,19]. The basic idea of these simulations is to count

the total number of sites or bonds in the backbones. For instance, for the percolation model in the ''bus-bar'' geometry, Grassberger [19] determined $X_b=0.3569(8)$. Slow convergence applies to X_b in this case. For the $q=2$ and 3 state Potts models, it has been estimated [18] that $X_b=0.25(1)$ and 0.25(2), respectively.

Another approach was taken by Jacobsen and Zinn-Justin [20] recently. They applied a transfer-matrix method, and obtained $X_b=0.3569(6)$ for the percolation model. Instead of the total number of sites in the backbones, they investigated the correlation length of *k*-connected clusters [21], where $k\geqslant 1$ is an integer. A cluster is considered to be *k*-connected if, by eliminating any $k-1$ sites or conducting bonds, no separation into disconnected subclusters is possible. This means that any two sites in the cluster are connected via *at least k* independent paths without any bond in common. At criticality, the behavior of these *k*-connected clusters is dominated by a family of exponents X_k. Moreover, it has been shown that $X_2=X_b$ [22], so that one can estimate X_b by studying 2-connected clusters.

In such transfer-matrix calculations, the finite system sizes are restricted to relatively small values, since the computer memory required increases exponentially with linear size L. For instance, in Ref. [20], L is limited to $2\leqslant L\leqslant 10$. This effect, together with the aforementioned slow finite-size convergence, makes it difficult to determine X_b accurately.

In this paper, we present another Monte Carlo study of the backbone exponents. However, in comparison with the earlier Monte Carlo studies [8,14,18,19], we apply a different sampling procedure. As mentioned above, the earlier methods involve counting procedures for the number of sites or bonds in the backbone. In other words, for a cluster of interest, all dangling bonds have to be identified and excluded. This appears to be a time-consuming task. Instead, in the present work, we sample the probability $P_2(r)$ that a pair of sites, separated by a distance *r*, are connected via *at least* two independent paths. For later convenience, we shall refer to the quantity $P_2(r)$ as the ''backbone correlation function.'' The sampling procedure for $P_2(r)$, which will be described in detail later, has a speed at least of the same order as the well-known Wolff cluster method [23]. We note that, in comparison with Refs. [8,14,18,19], our procedure to sample $P_2(r)$ is more in line with that used in Ref. [20].

The sampling procedure for $P_2(r)$ can be applied to the general *q*-state Potts model with any value of $q\geqslant 0$. Further, with this technique, we simply investigate systems with periodic boundary conditions rather than in the bus-bar geometry [8,18,19]. Thus, one avoids any finite-size correction associated with the surfaces in the bus-bar geometry. This will be confirmed later.

In the present work, several critical and tricritical *q*-state Potts systems are investigated. The values of *q* are chosen as $q=2-\sqrt{3}$, 1, 2, 3, and 4 for the critical systems, and $q=1$ and 2 at tricriticality. The critical $q=1$ and 2 Potts models are just the bond percolation and the Ising model, respectively, and the tricritical $q=2$ system is the Blume-Capel model [24,25]. For $q=4$, we avoid slow finite-size convergence by investigating a dilute $q=4$ Potts model and the Baxter-Wu model [26].

For these systems, extensive simulations were performed to determine X_b. In order to suppress critical slowing down, we make use of various efficient cluster Monte Carlo algorithms. For instance, for the dilute $q=4$ Potts and the Blume-Capel model, a geometric cluster method [27] was used to move vacancies on lattices. Another example is the simulation of the critical $q=2-\sqrt{3}$ Potts model. For this purpose, we formulate a Monte Carlo method for the Potts model with noninteger $q>0$. This method hardly suffers from critical slowing down for small $q>0$.

The outline of this paper is as follows. Section II reviews the Potts model and the systems included in the present paper. In Section III, the Monte Carlo simulations and the sampling procedures for P_2 are presented. In Sec. IV, the exact value of X_b is derived for the $q\to 0$ limit, and the numerical results for other values of *q* are presented. A short discussion is given in Sec. V.

II. MODELS

We start from the Hamiltonian of the dilute *q*-state Potts model on the square lattice [3], which reads

$$\mathcal{H}/k_{\mathrm{B}}T=-K\sum_{\langle i,j\rangle}\delta_{\sigma_i,\sigma_j}(1-\delta_{\sigma_i,0})-D\sum_{k}\delta_{\sigma_k,0}$$

$$(\sigma=0,1,\ldots,q). \tag{1}$$

Each site is occupied by a Potts variable with $\sigma=1,\ldots,q$ or by a vacancy $\sigma=0$, and the sum $\langle\,\rangle$ is over all nearest-neighbor sites. The abundance of the vacancies is controlled by the chemical potential *D*. Nonzero couplings *K* occur only between equal Potts variables, i.e., variables with nonzero values of σ.

Just as the ''pure'' Potts model, this model can be represented by Kasteleyn-Fortuin (KF) clusters [2,28], with each site of the lattice also occupied by a vacancy or a Potts variable. A nearest-neighbor bond is placed between each pair of equal, nonzero Potts variables with the probability $p=1-\exp(-K)$. We emphasize that, for any pair of nearest-neighbor sites, no bond is present if any of them is a vacancy. The whole lattice is then decomposed into clusters, i.e., the aforementioned KF clusters. This model is also referred to as a random-cluster model with a partition sum

$$Z=\sum_{\{v,b\}}u^{n_b}q^{n_c}w^{n_v}\quad(u=e^K-1\text{ and }w=e^D), \tag{2}$$

where the sum is over all mutually consistent vacancy and bond configurations, and n_b, n_c, and n_v are the total number of bonds, KF clusters, and vacancies, respectively. According to finite-size scaling, the average size of these KF clusters at criticality is governed by the magnetic scaling dimension X_h. With the partition sum (2), the Potts model is now also well defined for any noninteger $q\geqslant 0$.

For $D=-\infty$, the vacancies are excluded, and the system reduces to the pure Potts model. In this case, the model is self-dual, and the critical point follows [3] as $u_c=\exp(K_c)$

$-1=\sqrt{q}$ on the square lattice. With sufficiently abundant vacancies, tricritical systems, described by Eqs. (1) and (2), can be obtained.

Apart from these KF clusters, we also investigate so-called ''Potts'' clusters [9,10,13], defined as sets of Potts variables in the same state, connected by nearest-neighbor bonds. In other words, conducting bonds are *always* present between nearest-neighbor Potts variables as long as they are in the same state. Exponents describing Potts clusters are normally different from those for KF clusters. For instance, the $q=2$ Potts clusters, i.e., Ising clusters, are described by the magnetic exponent of the tricritical $q=1$ Potts model [9,10,29], different from that of the critical Ising model. Exponents for $q=3$ and $q=4$ Potts clusters have also been predicted as $X_h=7/80$ and $1/8$ [13].

Among the systems included in the present work, most of the systems can be described by Eqs. (1) or (2), except the Blume-Capel, and the Baxter-Wu model, which will be described later.

For the $q=4$ Potts model, logarithmic corrections arise due to the marginal field associated with the fugacity of vacancies [3]. In order to avoid such corrections, we investigate a dilute system at the point where this marginal field vanishes. We shall refer to this point, although somewhat imprecisely, as the ''fixed'' point. By means of a transfer-matrix calculation [30], we locate this fixed point as $K_{tc}=1.457\,90(1)$, $D_{tc}=2.478\,438(2)$, and $\rho_{tc}=0.212\,07(2)$ for the vacancy density. The precision of this result is considered sufficient for our later investigation of the backbone exponents.

For the case of $q=4$, beside the aforementioned dilute system, we also investigate the Baxter-Wu model [26], which is defined on the triangular lattice as

$$\mathcal{H}/k_{\mathrm{B}}T=-K\sum_{\Delta,\nabla}\sigma_i\sigma_j\sigma_k \quad (\sigma=\pm 1), \tag{3}$$

where the sum is over every up- and down-triangular face of the lattice. It has been shown that this model belongs to the universality class of the $q=4$ Potts model, and that logarithmic corrections are absent [26]. This means that the Baxter-Wu model also sits at the aforementioned fixed point. The critical point is given by $K_c=\ln(1+\sqrt{2})/2$ [26].

For the Ising and the Blume-Capel model, instead of Eq. (1), the Hamiltonian reads

$$\mathcal{H}/k_{\mathrm{B}}T=-K^{(I)}\sum_{\langle i,j\rangle}\sigma_i\sigma_j+D^{(I)}\sum_k\sigma_i^2 \quad (\sigma=-1,0,1), \tag{4}$$

where vacancies are also denoted as $\sigma=0$. We mention that, instead $p=1-\exp(-K)$, the bond probability for the KF clusters is now $p=1-\exp(-2K^{(I)})$. Analogously, for the chemical potential $D^{(I)}=-\infty$, the system reduces to the pure Ising model, with the critical point at $K_c^{(I)}=\ln(1+\sqrt{2})/2$. By means of a transfer-matrix calculation [30], we locate, with a sufficient precision, the tricritical point of the Blume-Capel model as $K_{tc}^{(I)}=1.643\,175\,9(1)$, $D_{tc}^{(I)}=3.230\,179\,7(2)$, and $\rho_{tc}=0.454\,950\,6(2)$.

III. ALGORITHMS

The Monte Carlo investigation of the backbone exponents of the aforementioned systems involves two parts, i.e., the simulation and the sampling procedure.

A. Monte Carlo simulations

For pure Potts systems with integer q, one can simply use the standard Wolff procedure [23]. In the present paper, these systems include the bond percolation, the Ising, and the $q=3$ Potts model. For the dilute systems, i.e., the Blume-Capel and the $q=4$ Potts model, cluster algorithms to flip between vacancies and Potts variables are generally not available. For this reason, we fix the global vacancy density at its equilibrium value, so that critical slowing down due to fluctuations in the number of vacancies is avoided. Cluster steps satisfying this conservation law are realized by a geometric cluster algorithm [27]. It moves groups of vacancies and Potts variables over the lattice in accordance with the Boltzmann distribution. This geometric cluster method is based on spatial symmetries, such as the spatial inversion symmetry. A detailed account can be found in Ref. [27].

Simulations of the Baxter-Wu model [26], which involves three-spin interactions, can be performed as follows [31]. The triangular lattice is divided into three sublattices, one of the sublattices is randomly chosen, and its spins are ''frozen.'' Since each elementary triangle contains one spin from each sublattice, only two-spin interactions remain effectively. Further, the Hamiltonian (3) is unchanged if all spins on these two sublattices are flipped. Due to this symmetry, one can now apply the Wolff cluster method on these two sublattices.

For the $0<q<1$ Potts model, we formulate a Monte Carlo method on the basis of the random-cluster representation, Eq. (2), which uses bond variables $l=0$ or 1. For simplicity, we illustrate this method precisely at the critical point $u_c=\sqrt{q}$.

(1) Randomly choose a bond variable l, connecting sites i and j.

(2) Draw a uniformly distributed random number $0\leqslant r\leqslant 1$.

(a) If $r<\sqrt{q}/(1+\sqrt{q})$, the edge l is occupied by a bond, i.e., $l=1$.

(b) If $r>1/(1+\sqrt{q})$, no bond is present at the edge l, i.e., $l=0$.

(c) If $\sqrt{q}/(1+\sqrt{q})\leqslant r\leqslant 1/(1+\sqrt{q})$, set $l=0$, and check whether sites i and j are connected. If they are not $l=1$; otherwise $l=0$.

(3) Current Monte Carlo step is completed, and goto (1).

Figure 1 illustrates possible connectivities of sites i and j and their relative weights. According to the procedure described above, the transition probability from (1) to (2) is $T_{1\to 2}=\sqrt{q}/(1+\sqrt{q})$, and that from (2) to (1) is $T_{2\to 1}=1/(1+\sqrt{q})$. Since equilibrium statistics implies that the probability p_1/p_2 is $1/\sqrt{q}$, one has $p_1T_{1\to 2}=p_2T_{2\to 1}$. Thus, the condition of detailed balance is satisfied between states (1) and (2). The same argument applies to states (3) and (4).

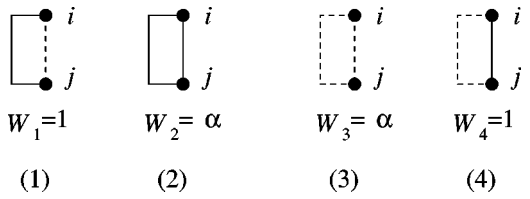

FIG. 1. Relative weights of the bond variables between neighboring sites i and j for the critical Potts model. Existing paths or bonds are represented by solid lines, while dashed lines mean that no path or bond is present. The relative weights between states (1) and (2) and those between (3) and (4) are specified as W_i with $\alpha=\sqrt{q}$.

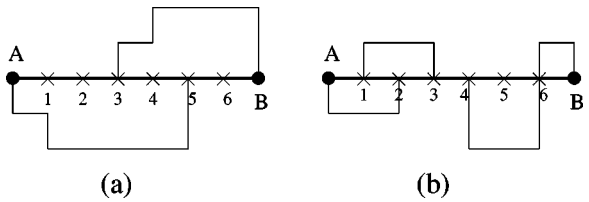

FIG. 2. Outline of the procedure to determine the connection variable C. The path $\mathbb{W}$ is shown as the thick line, and the remaining conducting bonds are shown as the thin lines. The bonds on $\mathbb{W}$ are temporarily eliminated first. In (a), the remaining path stops at 5. After the bonds between A, 1, . . . , and 5 are restored, the path connects to B, so that $C=2$. In (b), the bond between 3 and 4 is a red bond, and thus the path stops at site 3, so that $C=1$.

For small values of q, we observe that this method hardly suffers from critical slowing down. A similar procedure for $q>1$ has already been published [32]. Using the procedure described in Ref. [32], we simulated the $q=2+\sqrt{3}$ Potts model. In this case, we did observe serious critical slowing down, in agreement with the Li-Sokal bound [33] for the dynamic exponent. This is due to the rather strong energy fluctuations for $q>2$, especially when the marginal case $q_c=4$ is approached. In Ref. [32], this Monte Carlo technique was used to locate the marginal value of q_c in three dimensions, and it was claimed that no critical slowing down occurs. This stands, however, in a remarkable contrast with our findings near $q_c=4$ in two dimensions.

B. Sampling procedure

Here, we illustrate, in the language of the bond percolation model, the sampling procedure of the backbone correlation function $P_2(r)$.

Step 1, form a KF cluster. We shall illustrate the construction of a KF clusters as follows. Suppose a percolation model is defined on a $L\times L$ square lattice with periodic boundary conditions, and there are two sites A and B separated by a distance $L/2$. The task of this step is to form a KF cluster $\mathbb{F}$ from site A, and then to check whether B is also included in $\mathbb{F}$, so that A and B are connected via conducting bonds. For the Potts model with integer q, the sites in this KF cluster just form the Wolff cluster [23]. In the standard Wolff algorithm, if two nearest-neighbor sites are already in the cluster, it is not necessary to check whether the bond between them is present or absent. However, we are interested in the backbone correlation function here. If A and B are connected, one then asks how many mutually independent paths exist between A and B. Thus, all edges between nearest-neighbor sites within $\mathbb{F}$ have to be checked. We introduce a variable $C=0,1$, and 2, representing that there is no path, only one path, and *at least* two mutually independent paths between A and B, respectively. First, the edge variables on the lattice are initialized as $e_i=-1$ with $1\leqslant i\leqslant 2L^2$. The value $e_i=1$ represents that the ith edge is occupied by a bond, and $e_i=0$ stands for an empty edge. Since only one KF cluster is formed, not all edges of the square lattice are necessarily visited during the formation of $\mathbb{F}$. The edges, which are not visited, keep their value $e_i=-1$. After this initialization, uniformly distributed random numbers are drawn for each edge connecting to a neighbor in the same state. The edge is occupied by a bond if $r\leqslant p_c$ and is empty if $r>p_c$. The sites connected via these bonds are included in $\mathbb{F}$, as stored in a stack memory $\mathbb{S}$. Next, a site j is read and erased from $\mathbb{S}$. Then, the edges connecting to site j are checked. If they have not been visited ($e_i=-1$), new random numbers are used to determine whether they are occupied. Repetition of this procedure creates a list of occupied edges and sites, and thus a cluster $\mathbb{F}$ is formed. The determination of the backbone between A and B indeed requires that each bond between sites in $\mathbb{F}$ is visited. This procedure costs some additional computer time in comparison with the algorithm growing a Wolff cluster [6].

If the site B is not in the cluster $\mathbb{F}$, i.e., A and B are not connected, one has $C=0$, and the current Monte Carlo step is completed; otherwise, it continues as follows.

Step 2, a path $\mathbb{W}$ *is formed between* A and B. This can be done by an ''ant'' walking from A through the conducting bonds. Suppose the ant is currently at site j, it continues its journey by randomly choosing a conducting bond connecting to j, excluding the one it just passed. The ant does not pass a bond twice unless it arrives at a ''dead'' end. The dead end is defined as a site whose connected nearest-neighbor sites have all been visited. In this case, the ant walks back along the ''old'' road until it finds a ''new'' bond which it has not visited. Since site B is also in $\mathbb{F}$, the ant will always arrive at site B. The aforementioned path $\mathbb{W}$ is just composed of the bonds through which the ant has passed once and only once. An example is shown in Fig. 2(a), where the path $\mathbb{W}$ is represented by the thick solid line, and the sites on it are specified as $1,2,\ldots,n$.

The next task is to check whether there is any red bond on $\mathbb{W}$. If only one independent path can be formed between A and B, then *at least* one red bond occurs on the path $\mathbb{W}$. Furthermore, if any of these bonds is cut off, the ant cannot arrive at site B. An inefficient way is as follows. Temporarily eliminate a bond b on $\mathbb{W}$, and then let the ant restart its journey. If the ant can still arrive at B, the bond b cannot be a red bond, and thus is restored. Suppose all the bonds on the path $\mathbb{W}$ pass this test, then no red bond occurs between A and B, so that $C=2$; otherwise, $C=1$. In this way, however, the ant may become too tired to walk. Therefore, we apply a more efficient procedure.

Step 3, temporarily eliminate all the bonds on $\mathbb{W}$*, and let the ant restart its journey from A* to *B*. Suppose the ant cannot arrive at *B*; this does not necessarily mean, however, that there are red bonds. For instance, in Fig. 2(a), after the elimination of the whole path, the ant can only arrive at site 5. This indicates that the bonds between $A,1,\ldots,$ and 5 are not red bonds, and may thus be restored. Then, the ant continues its journey and arrives at *B*. In this case, no red bond occurs on the path $\mathbb{W}$, and $C=2$. An example of opposite case is given in Fig. 2(b). Following the same steps the ant cannot go beyond site 3, since the bond between sites 3 and 4 is a red bond. In this case, one has $C=1$.

In practical applications of this procedure, one can still improve the efficiency by some tricks. For instance, during the formation of the path $\mathbb{W}$, the site *B* may act as an ''attractor,'' so that $\mathbb{W}$ will not go too far from *B* and the ant need not continue its journey randomly. Furthermore, after the elimination of $\mathbb{W}$, instead of having the ant restart the journey, one can form a new cluster from *A* on the basis of the remaining bonds, and then check whether it includes *B*. In the case that *B* is not included, one restores the ''temporarily eliminated'' bonds on $\mathbb{W}$ which connect sites in *A*, and then continues to grow cluster *A*. This procedure ends when either *B* is included or no growth of *A* is possible. This avoids the situation that the ant has to walk back from a dead end.

With the connection variable *C*, the normal magnetic correlation function P_1 and the backbone correlation function P_2 between sites *A* and *B* can be defined as

$$P_1=\langle 1-\delta_{C,0}\rangle, \qquad P_2=\langle \delta_{C,2}\rangle, \tag{5}$$

where the symbol $\langle\ \rangle$ means the statistical average.

Efficiency of the sampling procedure. As described above, the sampling of P_2 involves up to three steps; the probability that steps 2 and 3 are performed is just the magnetic correlation function P_1. Step 1 is just a standard Wolff step with a small amount of added computer time, as mentioned above. Steps 2 and 3 involve a number of sites with an upper limit equal to the size of the cluster $\mathbb{F}$, so that their computer time is also of the same order as the Wolff step. Moreover, the probability P_1 that they are performed decays as L^{-2X_h}, and each sample is only taken between several simulation steps. As a result, the sampling procedure requires less computer time than the Wolff method. As an illustration, we performed 10^5 Monte Carlo steps for the percolation model with system size $8\leqslant L\leqslant 800$. We sampled the ratio *r* between the computer time for steps 2 and 3 and the total time, i.e., for steps 1, 2, and 3. The data for *r* are shown in Fig. 3 versus $L^{2X_h}=L^{-5/24}$. The approximate linearity indicates that the fraction of the computer time needed by the sampling procedure over the total time goes to 0 as $L\to\infty$.

IV. RESULTS

As mentioned in Sec. I, the backbone correlation function P_2, and thus the backbone exponent, is related with the behavior of the red bonds. For critical Potts models $0\leqslant q\leqslant 4$, the value of X_r is known to increase with *q*, which indicates

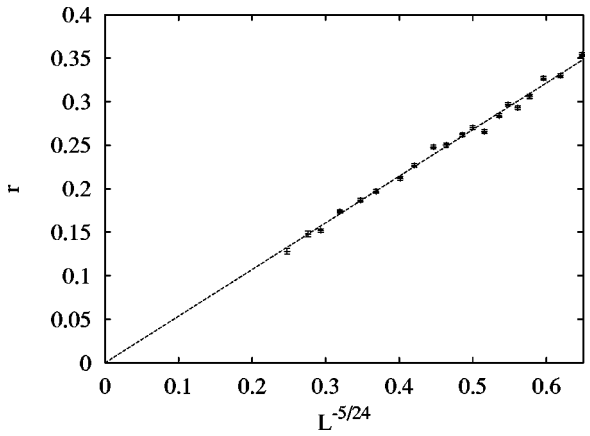

FIG. 3. The ratio *r*, between the computer time for steps 2 and 3 and the total time (steps 1, 2, and 3 combined), vs $L^{-5/24}$ for the percolation model. Every data point involves 10^5 Monte Carlo sweeps, and the system sizes are in the range $8\leqslant L\leqslant 800$. The ratio *r* extrapolates to 0 for $L\to\infty$.

that the KF clusters become less and less ramified. As a result, the backbone correlation function P_2 behaves more and more in line with P_1, so that X_b may be expected to approach the normal magnetic exponent X_h as $q\to 4$. For the tricritical Potts model, since $X_r\geqslant 2$, we expect that the backbone exponent X_b reduces to the magnetic exponent X_h.

For the critical $q\to 0$ Potts model [3,2], the KF clusters span the whole lattice without any loop, and are thus referred to as spanning trees. In this case, between any pair of points on the lattice, there is precisely only one path $\mathbb{P}$, so that the backbone correlation function P_2 vanishes. This is due to the vanishing of the amplitude of P_2 as $q\to 0$. As a consequence, one cannot obtain $X_b(q\to 0)$ by investigating *k*-connected clusters, as we will do for other values of $q>0$. In this case, one can simply make use of the original definitions of the geometric quantities in Sec. I, which include the backbone, the red bond, and the chemical-path exponents. From these definitions, one knows that the aforementioned path $\mathbb{P}$ is just the chemical path, and that the backbone precisely consists of all the bonds on $\mathbb{P}$. Furthermore, all these bonds are red bonds. Since the red-bond scaling dimension is exactly known $X_r=3/4$ [9,34], one simply has that $X_2=X_b=X_{\min}=3/4$ for $q\to 0$. In fact, the statement that $X_b=X_r=X_{\min}$ holds for any type of spanning tree.

In the remaining part of this section, we present our Monte Carlo determinations of X_b for the systems discussed in Sec. II. Periodic boundary conditions apply to all these systems. The aforementioned site *A* was chosen at random, and site *B* is chosen at a distance $r=L/2$ in the *x* direction from *A*. Further, we chose a site *D* also separated from *A* a distance $L/2$ but in the *y* direction.

The correlation functions P_1 and P_2 were sampled both in the *x* and *y* directions, such that $P_1=[P_1^{(x)}+P_1^{(y)}]/2$ and $P_2=[P_2^{(x)}+P_2^{(y)}]/2$. Moreover, we sampled another backbone correlation function P_{22} that *A* is simultaneously connected to *B* and *D* by *at least* two mutually independent paths.

According to finite-size scaling, the quantities P_1, P_2, and P_{22} behave at criticality as

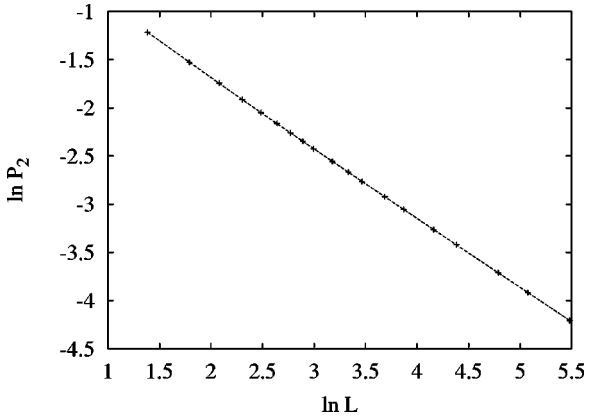

FIG. 4. Decay of the backbone correlation function P_2 for KF clusters of the critical bond percolation model. The data are shown as $\ln P_2$ vs. $\ln L$.

$$P_1 = L^{-2X_h}(a_0 + a_2 L^{y_i} + a_3 L^{-2} + a_4 L^{-3}), \quad (6)$$

$$P_2 = L^{-2X_b}(b_0 + b_1 L^{y_{ib}} + b_2 L^{y_i} + b_3 L^{-2} + b_4 L^{-3}), \quad (7)$$

and

$$P_{22} = L^{-3X_b}(c_0 + c_1 L^{y_{ib}} + c_2 L^{y_i} + c_3 L^{-2} + c_4 L^{-3}), \quad (8)$$

where y_i is the exponent of the leading irrelevant thermal scaling field, and we have assumed integer correction exponents (of $1/L$). The amplitudes a_i, b_i, and c_i are unknown constants. In comparison with the magnetic correlation function P_1, the geometric quantities P_2 and P_{22} may be expected to suffer from additional finite-size corrections, with unknown associated exponents y_{ib}. More rapidly decaying corrections are neglected here. The unknown amplitudes and exponents are determined from multivariate least-squares analysis using the Levenberg-Marquardt method [35]. For the systems in the present work, the values of X_h, obtained from the fits of P_1, are all in excellent agreement with their exact results [11], and need not be discussed in this work.

The bond percolation model. For this model, the system sizes L were taken in the range $8 \leqslant L \leqslant 240$. The data for P_2 are shown in Fig. 4, and do not indicate the presence of large finite-size corrections. Equation (7) was fitted to the Monte Carlo data according to the least-squares criterion, and the exponent y_{ib} was left as a free parameter. We observed that the terms with amplitudes b_2, b_3, and b_4 do not decrease the residual χ^2, and thus they were not included in the fit. We obtain $X_b = 0.3566(2)$ and $y_{ib} = -1.27(4)$, where the error bars are twice the statistical standard deviations. Compared to Ref. [19], it seems that our Monte Carlo data suffer less seriously from finite-size corrections. This may be due to our choice of a geometry with periodic boundary conditions instead of the bus-bar geometry. For clarity, we plot the value of $P_2 L^{2X_b} - b_0$ as a function of $L^{-1.27}$ in Fig. 5, where $X_b = 0.3566(2)$ and $b_0 = 0.742(2)$ are taken from the fit. The apparent linearity indicates that, indeed, finite-size corrections of P_2 can be well accounted for by a single power law $b_1 L^{y_{ib}}$.

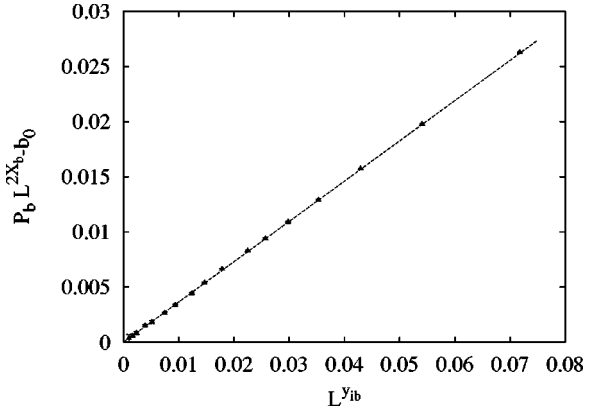

FIG. 5. Finite-size corrections in P_2 for KF clusters of the critical bond percolation model, shown as $P_2 L^{2X_b} - b_0$ vs $L^{y_{ib}}$. The values of X_b, b_0, and y_{ib} are taken from the numerical fit: $X_b = 0.3566(2)$, $b_0 = 0.742(2)$, and $y_{ib} = -1.27(4)$.

The Ising model and the tricritical $q=1$ Potts model. The simulations were performed for critical Ising systems on square lattices in the range $6 \leqslant L \leqslant 240$. The quantities P_2 and P_{22} were sampled both for KF and Ising clusters. As mentioned above, the Ising clusters are described by the magnetic dimension $X_h = 5/96$ of the tricritical $q=1$ Potts model [9,10,29]. The Monte Carlo data for P_2 of the KF clusters are shown in Fig. 6, which indicates that $2X_b \approx 0.54$. Equations (7) and (8) were simultaneously fitted to P_2 and P_{22}, respectively, so that X_b and y_{ib} appear in the fit only once. In addition to the terms with y_{ib}, the fit also included a correction with $y_i = -2$. We obtain $X_b = 0.2696(3)$ and $y_{ib} = -0.87(4)$ for KF clusters, and $X_b = 0.0520(3)$ for Ising clusters. Here, the error bars are again two standard deviations. As expected, for the Ising clusters X_b is in a good agreement with $X_h = 5/96 = 0.5208\ldots$ of the tricritical $q=1$ Potts model.

The critical $q=3$ Potts model. The simulations were performed for the $q=3$ Potts model at criticality with system sizes L in the range $6 \leqslant L \leqslant 360$. The quantities P_2 and P_{22}

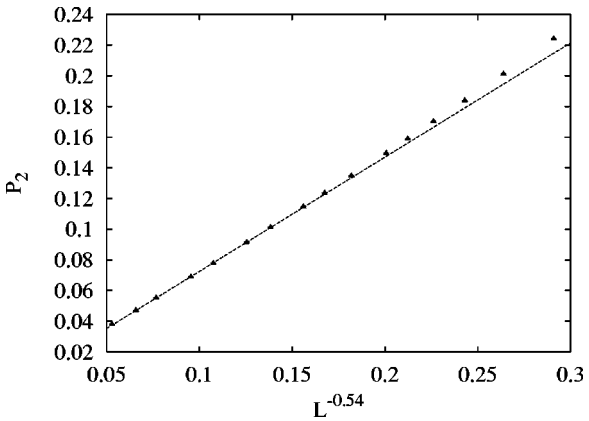

FIG. 6. Decay of the backbone correlation function P_2 for KF clusters of the critical Ising model. The data are shown as P_2 vs $L^{-0.537}$.

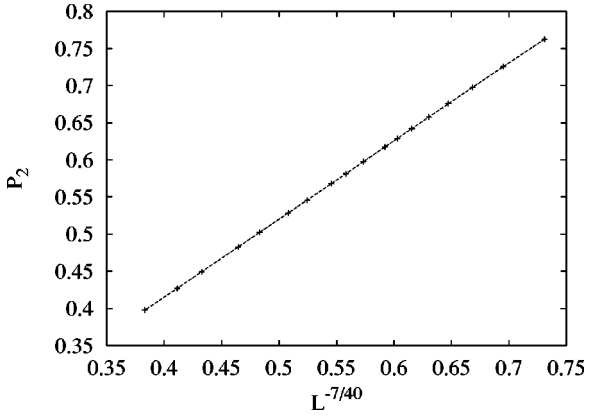

FIG. 7. Decay of the quantity P_2 for Potts clusters of the critical $q=3$ Potts model. The data are shown as P_2 vs $L^{-7/40}$.

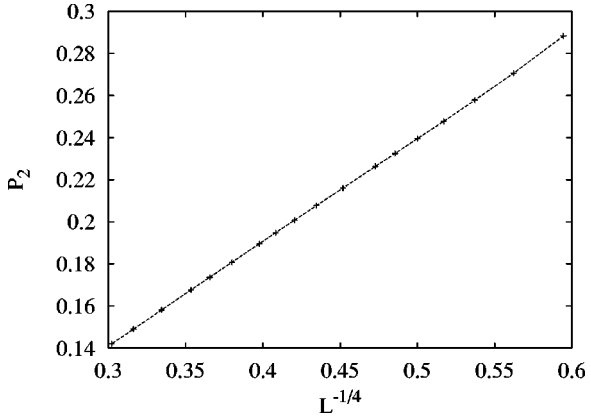

FIG. 8. Decay of the quantity P_2 for the KF clusters of the dilute $q=4$ Potts model. The data are shown as P_2 vs $L^{-1/4}$.

were sampled both for KF and Potts clusters. As mentioned above, the exponent for the Potts clusters has been predicted as $X_h=7/80$ [13]. As a test, Eq. (6) was fitted to the data for P_1, and we obtain $X_h=0.0876(2)$, in good agreement with 7/80. Furthermore, a plot of the data for P_{22} for Potts clusters in Fig. 7 also indicates $X_b \approx 7/80$. Again, Eqs. (7) and (8) were simultaneously fitted to P_2 and P_{22}, respectively. For the $q=3$ Potts model, the correction term with $y_i=-4/5$ [12] appears difficult to separate from that with y_{ib}, and thus it was neglected in the fit. The corrections with L^{-2} were included, and the fit yields that $X_b=0.2105(5)$ and $y_{ib}=-0.61(4)$ for the KF clusters, and that $X_b=0.0873(3)\approx X_h=7/80$ for the Potts clusters.

The tricritical Blume-Capel model. As mentioned above, the backbone exponent X_b for the tricritical $q=1$ Potts model has already been determined from the Ising clusters. The result $X_b=0.0520(3)\approx 5/96$ indicates that X_b reduces to the magnetic exponent X_h for tricritical Potts models. As an independent test, we directly Monte Carlo simulated the tricritical Blume-Capel model. The simulations use the fixed-vacancy-density ensemble, as discussed in Sec. II. The system sizes were taken in the range $10 \leqslant L \leqslant 360$, and both quantities P_2 and P_{22} were sampled. The numerical fits yield $X_b=0.0760(8)$ and 0.0753(4) for the KF and the Potts cluster, respectively. Both are in good agreement with the tricritical magnetic exponent $X_h=3/40$ [11,12].

The Baxter-Wu and the tricritical $q=4$ Potts model. The $q=4$ Potts model is a marginal case, not only because the second-leading thermal exponent $X_{t2}=2$, but also because that the red-bond exponent $X_r=2$ [9,13]. Thus, the bond-dilution scaling field, conjugate to the red bonds, becomes marginal, and the question arises whether this field is marginally relevant or irrelevant for critical KF and Potts clusters. As independent tests, Monte Carlo simulations were performed both of the aforementioned dilute $q=4$ Potts model at the fixed point and the Baxter-Wu model. For the latter, the system size L was taken as multiples of 6 and in the range $12 \leqslant L \leqslant 240$. For the dilute $q=4$ model, the system sizes were in the range $10 \leqslant L \leqslant 360$. The Monte Carlo data for P_2 of the KF clusters, shown in Fig. 8, indicate that $2X_b \approx 1/4$. For these two models, logarithmic finite-size corrections are absent for ''thermodynamic'' quantities such as the magnetic correlation P_1. However, we have no solid reason to assume that such logarithmic corrections are absent for geometric quantities such as P_2. Thus, at criticality, we assume that, instead of Eqs. (7) and (8), P_2 behaves as

$$P_2 = L^{-2X_b}(b_0 + b_1/\ln L + b_2/\ln^2 L + b_3/L^2). \qquad (9)$$

Equation (9) was fitted to the Monte Carlo data for these two models simultaneously. On the basis of the χ^2 criterion, we applied a cutoff for small system sizes $L \leqslant 12$. We then ob-

TABLE I. Results for the backbone exponent X_b and the associated correction-to-scaling exponent y_{ib} for critical Potts systems. Estimated error margins in the last decimal place, which are twice the standard deviations in the fits, are shown in parentheses. For comparison, the magnetic dimensions X_h and estimations of X_b by other sources are also listed (X_b^*, last column). The numbers given as fractions are exact.

g	Model	X_h	X_b	y_{ib}	X_b^*
2	$q=0$ Potts	0	3/4		
7/3	$q=2-\sqrt{3}$ Potts	11/168	0.4953(3)	$-2.3(2)$	
8/3	Percolation	5/48	0.3566(2)	$-1.27(4)$	0.3569(6) [20]
3	Ising	1/8	0.2696(3)	$-0.87(4)$	0.25(2) [18]
10/3	$q=3$ Potts	2/15	0.2105(5)	$-0.61(4)$	0.25(2) [18]
4	$q=4$ Potts	1/8	0.127(4)	$1/\ln L$?	

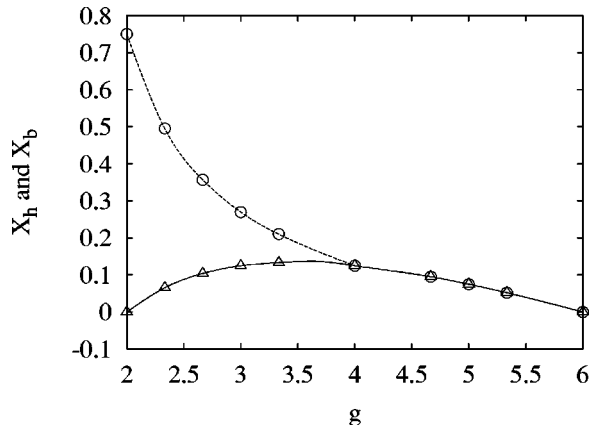

FIG. 9. The backbone and the magnetic scaling dimension, X_b and X_h, as a function of the coupling constant of the Coulomb gas g. The symbols $\triangle$ and $\bigcirc$ represent X_h and X_b, respectively. The tricritical branch of the Potts model corresponds with $4 \leqslant g \leqslant 6$; X_h and X_b coincide in this range.

tain that $X_b = 0.124(2)$ and $0.127(4)$ for the Potts and the KF clusters, respectively, in agreement with $X_h = 1/8$.

The critical $q = 2 - \sqrt{3}$ *Potts model*. As a case between $q = 0$ and 1, we simulated the $q = 2 - \sqrt{3}$ Potts model. The system sizes were taken in the range $6 \leqslant L \leqslant 200$, and the quantity P_2 was sampled. We find that, as expected, the finite-size corrections converge rapidly, so that Eq. (7) with only the first two terms is sufficient to describe the Monte Carlo data. To obtain a satisfactory χ^2 residual, we applied a cutoff for small system sizes $L < 8$. This leas to $X_b = 0.4953(3)$ and $y_{ib} = -2.3(2)$.

V. DISCUSSION

We have developed several Monte Carlo methods to determine the backbone exponents of the q-state Potts model. The efficiency of these methods is reflected by the precision of the numerical results, summarized in Table I, which significantly improves over existing results. We find that, for critical Potts models, the backbone scaling dimension X_b approaches the magnetic dimension X_h as $q \to 4$. This reflects the fact that Kasteleyn-Fortuin clusters become more and more compact with increasing q. Further, it has been confirmed numerically that, for the tricritical Potts model, the backbone exponent reduces to the magnetic exponent. In Fig. 9, we plot X_b and X_h as a function of the coupling constant of the Coulomb gas g [11]. The relation between g and q is given by $q = 2 + 2\cos(g\pi/2)$ [11], with $2 \leqslant g \leqslant 4$ and $4 \leqslant g \leqslant 6$ for the critical and tricritical Potts models, respectively.

The present Monte Carlo methods can also be applied in three dimensions, and simulations for the percolation and the Ising model are currently being performed [30].

ACKNOWLEDGMENTS

The authors are indebted to Dr. J. R. Heringa for valuable discussions. This research was supported by the Dutch FOM foundation (''Stichting voor Fundamenteel Onderzoek der Materie''), which is financially supported by the NWO (Nederlandse Organisatie voor Wetenschappelijk Onderzoek).

[1] R.B. Potts, Proc. Cambridge Philos. Soc. **48**, 106 (1952).
[2] P.W. Kasteleyn and C.M. Fortuin, J. Phys. Soc. Jpn. Suppl. **46**, 11 (1969); C.M. Fortuin and P.W. Kasteleyn, Physica **57**, 536 (1972).
[3] F.Y. Wu, Rev. Mod. Phys. **54**, 235 (1982).
[4] H. J Herrmann and H.E. Stanley, Phys. Rev. Lett. **53**, 1121 (1984).
[5] H. J Herrmann, D.C. Hong, and H.E. Stanley, J. Phys. A **17**, L261 (1984).
[6] D. Stauffer and A. Aharony, *Introduction to Percolation Theory* (Taylor & Francis, Philadelphia, 1994).
[7] M. Sahimi and S. Arbabi, J. Stat. Phys. **62**, 1873 (1990).
[8] P. Grassberger, J. Phys. A **25**, 5475 (1992), and references therein.
[9] A. Coniglio, Phys. Rev. Lett. **62**, 3054 (1989).
[10] H.W.J. Blöte, Y.M.M. Knops, and B. Nienhuis, Phys. Rev. Lett. **68**, 3440 (1992).
[11] B. Nienhuis, in *Phase Transitions and Critical Phenomena*, edited by C. Domb and J. L. Lebowitz (Academic Press, London, 1987), Vol. 11, p. 1, and references therein.
[12] J. L. Cardy, in *Phase Transitions and Critical Phenomena*, edited by C. Domb and J. L. Lebowitz (Academic Press, London, 1987), Vol. 11, p. 55, and references therein.
[13] C. Vanderzande, J. Phys. A **25**, L75 (1992).
[14] H. J Herrmann and H.E. Stanley, J. Phys. A **21**, L829 (1988).
[15] T.A. Larsson, J. Phys. A **20**, L291 (1987).
[16] H. Saleur, Nucl. Phys. B **382**, 486 (1992).
[17] G.F. Lawler, O. Schramm, and W. Werner, e-print math-PR/0108211.
[18] E.N. Miranda, Physica A **175**, 229 (1991).
[19] P. Grassberger, Physica A **262**, 251 (1999), and references therein.
[20] J.L. Jacobsen and P. Zinn-Justin, Phys. Rev. E **66**, 055102(R) (2002); J. Phys. A **35**, 2131 (2002).
[21] W. T. Tutte, *Graph Theory* (Cambridge University Press, Cambridge, England, 1984).
[22] G. Paul and H.E. Stanley, Phys. Rev. E **65**, 056126 (2002).
[23] U. Wolff, Phys. Rev. Lett. **62**, 361 (1989).
[24] M. Blume, Phys. Rev. **141**, 1517 (1966).
[25] H.W. Capel, Physica **32**, 966 (1966); **33**, 295 (1967).
[26] R.J. Baxter and F.Y. Wu, Phys. Rev. Lett. **31**, 1294 (1973); Aust. J. Phys. **27**, 357 (1974).
[27] J.R. Heringa and H.W.J. Blöte, Physica A **232**, 369 (1996); Phys. Rev. E **57**, 4976 (1998).
[28] A. Coniglio and F. Peruggi, J. Phys. A **15**, 1873 (1982).
[29] B. Nienhuis, J. Phys. A **15**, 199 (1982).

[30] Y. Deng and H. W. J. Blöte (unpublished).
[31] M. A. Novotny and H. G. Evertz, in *Computer Simulation Studies in Condensed-Matter Physics VI*, edited by D. P. Landau, K. K. Mon, and H.-B. Schüttler (Springer, Berlin, 1993), p. 188.
[32] F. Gliozzi, Phys. Rev. E **66**, 016115 (2002).
[33] X.J. Li and A.D. Sokal, Phys. Rev. Lett. **63**, 827 (1989).
[34] B. Duplantier, J. Stat. Phys. **54**, 581 (1989); Phys. Lett. B **228**, 379 (1989).
[35] See, e.g., W. H. Press, B. P. Flannery, S. A. Teukolsky, and W. T. Vetterling, *Numerical Recipes* (Cambridge University Press, Cambridge, 1986).